Spectroscopic probing of location and dynamics of an environment-sensitive intramolecular charge transfer probe within liposome membranes

ARTICLE *in* JOURNAL OF COLLOID AND INTERFACE SCIENCE · JULY 2011

Impact Factor: 3.37 · DOI: 10.1016/j.jcis.2011.07.074 · Source: PubMed

2 AUTHORS, INCLUDING:

Bijan Kumar Paul
Indian Institute of Science Education and R…

72 PUBLICATIONS **895** CITATIONS

SEE PROFILE

Journal of Colloid and Interface Science 363 (2011) 529–539

Contents lists available at ScienceDirect

Journal of Colloid and Interface Science

www.elsevier.com/locate/jcis

Spectroscopic probing of location and dynamics of an environment-sensitive intramolecular charge transfer probe within liposome membranes

Bijan Kumar Paul, Nikhil Guchhait *

Department of Chemistry, University of Calcutta, 92 A.P.C. Road, Calcutta 700 009, India

ARTICLE INFO

Article history:
Received 31 May 2011
Accepted 21 July 2011
Available online 28 July 2011

Keywords:
Intramolecular charge transfer
Liposome
Emission spectroscopy
Rotational relaxation dynamics
REES
Solvent-relaxation

ABSTRACT

The present work demonstrates the interaction of an intramolecular charge transfer (ICT) probe 5-(4-dimethylamino-phenyl)-penta-2,4-dienoic acid methyl ester (DPDAME) with liposome membranes of dimyristoyl-L-α-phosphatidylcholine (DMPC) and dimyristoyl-L-α-phosphatidylglycerol (DMPG) studied by steady-state absorption, emission and time-resolved emission techniques. A huge hypsochromic shift together with remarkable enhancement of fluorescence quantum yield of the polarity sensitive ICT emission of DPDAME upon interaction with the lipids has been rationalized in terms of incorporation of the probe into hydrophobic interior of the lipids. Compelling evidences for penetration of the probe into the hydrocarbon interior of the lipids have been deduced from intertwining different experimental results e.g., micropolarity in the immediate vicinity of the probe in lipid environments, steady-state anisotropy, red-edge excitation shift (REES), fluorescence quenching experiments and time-resolved measurements. The rotational relaxation dynamics study of the membrane-bound probe unveils the impartation of high degree of motional rigidity. Wavelength-selective emission behaviour paves way for monitoring of solvent-relaxation in the membranes. Overall, the ICT probe DPDAME displays its commendable sensitivity in deciphering the microheterogeneous environments of liposomal membranes of DMPC and DMPG and promises a new membrane-polarity sensitizing probe.

1. Introduction

Ever since the seminal report on intramolecular charge transfer (ICT) reaction in 4-N,N-dimethylamino benzonitrile (DMABN) by Lippert et al. [1], the study of ICT reaction in numerous organic compounds [2–6] has formed the nucleus of innumerable research activities over the years. Apart from its intriguing photophysics, the phenomenon of photo-induced ICT reaction garners attention even today with a view to its many-faceted applicative prospects such as, in their potential to serve as relatively simpler molecular systems in understanding the importance of photoinitiated electron transfer and charge transfer phenomena in many natural processes like photosynthesis and many photochemical reactions [7–9], in laser dyes, molecular switching devices, photochemical-energy conversion and so forth [8,10]. The characteristic solvent polarity dependent emission behaviour paves way for its viable exploitation as molecular reporter for probing complex biological and biomimicking environments [11–13] and also various supramolecular architectures [14,15]. Such spectroscopic properties of ICT probes has been welcome in biochemical research obviously because any simpler model having the ability to provide insights into complex biosystems can fathom deep into the understanding and deciphering many long-standing root-level problems.

Research in the field of membrane biochemistry has traditionally been concerned with the interaction of probe molecules with lipid membranes. Therefore, a marked advancement is noted in the study of incorporation of various fluorophores into liposome membranes in recent time with a view to gather a healthy score of information regarding the structure, dynamics and functioning of biological membrane systems [7,16–27]. Phospholipids are the fundamental matrix of natural membranes and correspond to the environments in which proteins, enzymes, drugs display their activity [16,21,22]. The wide diversity in composition and structure of biological membranes has promoted the use of synthetic liposomes or vesicles which have long been realized as authentic mimic of cell membranes on perspectives of its geometry, topology and structural skeleton [24–26,28–32]. Apart from this, the liposomes have also formed a potential avenue for research in such applicative fields as food industry, immunology, vehicle for targeted drug delivery and so forth [28,31–33].

The present work reports the interaction behaviour of an ICT probe DPDAME with the microheterogeneous environments of lipids. The probe DPDAME exhibits two broad and structureless absorption bands at ~370 nm and ~260 nm in water which were ascribed to $S_1 \leftarrow S_0$ and $S_n \leftarrow S_0$ ($S_2 \leftarrow S_0$ or higher) transitions, respectively [34]. The emission spectra of DPDAME exhibit charac-

* Corresponding author. Fax: +91 33 2351 9755.
E-mail address: nguchhait@yahoo.com (N. Guchhait).

0021-9797/$ - see front matter © 2011 Elsevier Inc. All rights reserved.
doi:10.1016/j.jcis.2011.07.074

teristic "anomalous" dual fluorescence in polar solvents of which a solvent polarity insensitive, weakly intense, higher energy local emission band is centred at ~425 nm and a lower energy but relatively intense charge transfer band is located at ~545 nm in water. This large Stokes shifted ($\Delta\nu$ = 8408 cm^{-1} in water) emission band arises from the CT state of DPDAME and thus experiences remarkable sensitivity to solvent polarity. Steady-state absorption and fluorescence spectroscopic study of DPDAME in solvents of different polarity clearly establish the phenomenon of ICT reaction in DPDAME [2–4,7,34]. The ICT process in the probe has been further substantiated through solvatochromic measurements based on Lippert–Mataga relationships [34]. The remarkable sensitivity of ICT emission of the probe, DPDAME on medium polarity as well as medium rigidity has been processed to delve into the microenvironments of the liposomal membranes of DMPC and DMPG. The results demonstrate the effect of lipid environments on steady-state fluorescence, anisotropy and time-resolved fluorescence decay properties of the entrapped fluorophore. Particular emphasis is focused on deciphering the location of the extrinsic molecular probe within the lipid environments. The present work also unveils the solvent-relaxation dynamics based on wavelength-selective emission approach. The rotational relaxation dynamics of the entrapped flurophore is also monitored by time-resolved fluorescence anisotropy decay measurements.

2. Experimental

2.1. Materials

5-(4-Dimethylamino-phenyl)-penta-2,4-dienoic acid methyl ester (DPDAME) (Scheme 1) was synthesized and purified following usual literature procedure and is described elsewhere [34]. It was repeatedly recrystallized from ethanol (EtOH) and the purity of the compound was established on TLC plate. DMPC and DMPG (Scheme 1) were procured from Sigma–Aldrich, USA and used as received. Tris buffer was purchased from SRL, India and solution (Tris–HCl buffer) of required pH (7.40) was prepared from this using deionized water from Milli-Q water purification system (Millipore). The concentration of DPDAME was maintained at 2.0 μM (by addition from a stock solution prepared in the aqueous buffer) and pH at 7.40 throughout the study. All solvents such as chloroform ($CHCl_3$) and methanol (CH_3OH) used were of UV Spectroscopic grade (Spectrochem, India).

2.2. Instrumentations and methods

2.2.1. Dynamic light scattering

Dynamic light scattering (DLS) measurements were carried out on a Malvern Nano-ZS instrument employing a 4 mW He–Ne laser (λ = 632.8 nm) and equipped with a thermostatted sample chamber. The sample was poured into a DTS0112 low volume disposal sizing cuvette of 1.5 mL (path-length 1 cm). The operating procedure was programmed by the DTS software in a fashion that there were average of 25 runs, each run being averaged for 15 s, and then a particular hydrodynamic diameter and a size distribution was evaluated.

2.2.2. Steady-state measurements

The absorption and emission spectra were acquired on Hitachi UV–Vis U-3501 spectrophotometer and Perkin–Elmer LS-55 fluorimeter, respectively.

The steady-state fluorescence anisotropy was recorded on Perkin–Elmer LS-55 fluorimeter. The steady-state anisotropy (r) is defined as [7]:

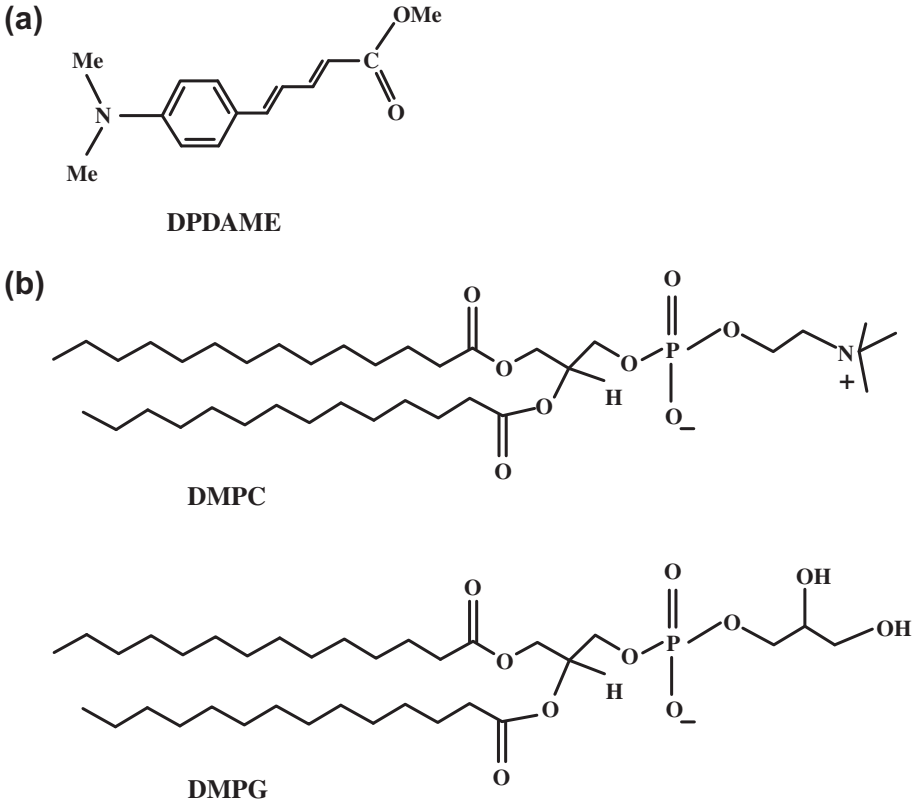

Scheme 1. Schematic of the structures of (a) DPDAME; (b) DMPC and DMPG.

$$r = \frac{(I_{VV} - G \cdot I_{VH})}{(I_{VV} + 2G \cdot I_{VH})} \quad (1)$$

$$G = \frac{I_{HV}}{I_{HH}} \quad (2)$$

where I_{VV} and I_{VH} are the emission intensities when the excitation polarizer is vertically oriented and the emission polarizer is oriented vertically and horizontally, respectively. G is the correction factor.

2.2.3. Time-resolved measurements

Fluorescence lifetimes were measured by a Time-Correlated Single Photon Counting (TCSPC) spectrometer using a diode laser (IBH, UK) as the light source at 370 nm to trigger the fluorescence of DPDAME and the signals were collected at the magic angle of 54.7° to eliminate contamination by contribution from fluorescence anisotropy decay [7] (typical instrument time resolution ~80 ps). The decays were deconvoluted on Data Station v-2.6 decay analysis software. The acceptability of the fits was evaluated on the basis of χ^2 criterion and a visual inspection of the residuals of the fitted functions to the data [2,3,7,16,33].

Mean (average) fluorescence lifetimes were calculated using the following equation [7]:

$$\langle \tau_f \rangle = \frac{\sum_i \alpha_i \tau_i^2}{\sum_i \alpha_i \tau_i} \quad (3)$$

in which α_i represents the amplitude corresponding to the ith decay time constant τ_i.

For time-resolved fluorescence anisotropy decay measurements, the polarized fluorescence decays for the parallel [$I_{||}(t)$] and perpendicular [$I_{\perp}(t)$] emission polarizations with respect to the vertical excitation polarization were first collected at the emission maxima of the probe (typical instrument time resolution ~80 ps). The anisotropy decay function $r(t)$ was constructed from these $I_{||}(t)$ and $I_{\perp}(t)$ decays using the following equation [7,14,16]:

$$r(t) = \frac{I_{||}(t) - G \cdot I_{\perp}(t)}{I_{||}(t) + 2G \cdot I_{\perp}(t)} \quad (4)$$

where G is the correction factor for the detector sensitivity to the polarization detection of the emission.

2.2.4. Calculation and methods

Fluorescence quantum yield (Φ_f) was determined using β-naphthol (Φ_f = 0.23 in methylcyclohexane) as the secondary standard in the following equation [2–4,7,33,34]:

$$\frac{\Phi_S}{\Phi_R} = \frac{A_S}{A_R} \times \frac{(Abs)_R}{(Abs)_S} \times \frac{n_S^2}{n_R^2} \quad (5)$$

where Φ is quantum yield, "*Abs*" is absorbance, A is area under the fluorescence curve and n is the refractive index of the medium. Subscripts "*S*" and "*R*" denote the corresponding parameters for the sample and reference, respectively.

All experiments have been performed at 310 K unless otherwise specified. During fluorescence quenching experiments addition of Ni^{2+} salt (from a stock solution in Tris–HCl buffer) was limited within 50 μL into a total volume of 2.5 mL of the solution under experiment, so as to eliminate the possibility of any significant volume change. Commercially available perchlorate salt of nickel, $Ni(ClO_4)_2(H_2O)_6$, has been used for quenching studies.

2.2.5. Deconvolution of fluorescence emission spectra

The fluorescence spectra were analyzed by deconvolution into overlapping Gaussian curves using the algorithm implemented in MS Origin 7 to obtain the minimum number of reproducible components using the adjustable parameters of the centre, width, and amplitude for the resolved bands. Multiple attempts to fit the data with different starting parameters provided a survey of the extent of statistically equivalent parameter sets. Comparing several deconvolutions of an overall spectrum, a "good" fit was then judged by several criteria including a minimum in the goodness-of-fit parameter χ^2 (the weighted sum of the squares of the deviations), and a maximum value for the square of the multiple correlation coefficient, r^2. From these statistically acceptable fits, a "good" fit is further judged by the reproducibility in the values for the centres of the Gaussian curves. A final, *albeit* subjective, criterion was to examine the fits for physically plausible results [35,36].

2.3. Preparation of liposome and its labelling

The method described in the literature was followed for preparation of lipids [37]. Briefly, appropriately weighed quantity of phospholipid was solubilized in 2:1 (v/v) mixture of $CHCl_3$:CH_3OH, from which thin films were deposited on the inner walls of a small fusion tube under a stream of dry nitrogen. The resulted film was dried in a vacuum desiccator overnight at 4 °C. The film was then solubilized in Tris–HCl buffer (at pH 7.4 containing 20 mM NaCl [16]) followed by vortexing to disperse the lipid. The dispersion was then sonicated for 40 min using Bransonic 1510E-DTH sonicator. The resulted solution was then centrifuged (Spinwin, MC-02) at 10,000 rpm for 10 min to remove foreign particles, if any. The size and size distribution of the lipids were extracted from dynamic light scattering (DLS) experiment which provides an effective way to investigate the dimensions of macromolecular and supramolecular assemblies. Under the presently employed experimental conditions, the present lipid systems DMPC (1 mM) and DMPG (1 mM) exhibited fairly monomodal distribution with an average diameter of 34 ± 3 nm for DMPC and 17.7 ± 3 nm for DMPG (Fig. 1), indicating the formation of small unilamellar vesicles in both cases. The diameters obtained in the present case are consistent with recent literature reports [38,39]. Concentrations of lipids for DLS measurements were chosen from saturation of the DPDAME–lipid interactions as revealed from fluorometric experiments to be discussed in the forthcoming sections (Results of DLS measurements with other concentrations of both the lipids (0.75 mM and 1.5 mM) were consistent within the experimental error limit). It is noted that the widths of the size distribution profiles for DMPC and DMPG lipids are different (Fig. 1) reflecting their varying degrees of polydispersities. The polydispersity (Pd), which is a measure of the particle size distribution width, was evaluated from the equation: $Pd = (\sigma/d_h) \times 100\%$ [40], in which σ is the standard deviation of the distribution and d_h is the mean

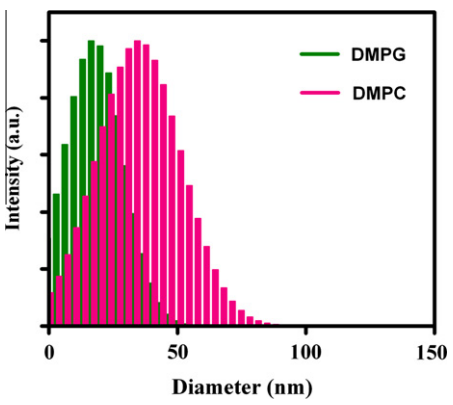

Fig. 1. Size (diameter) distribution graph for 1 mM DMPC and 1 mM DMPG in aqueous buffer solution at pH 7.4.

hydrodynamic diameter as obtained from DLS size distribution graph. The calculated values, according to the above equation, indicate polydispersity (Pd) of 8.82% for DMPC lipid and 16.95% for DMPG lipid.

All experiments have been performed with only freshly prepared solutions. Solutions for spectral background correction have been prepared the same way except that the probe was omitted.

Table 1
Simplified summary of the modulated photophysics of DPDAME upon interaction with the lipids as obtained from steady-state spectroscopic measurements.

Environment	λ_{abs} (nm)	λ_{em} (nm)	K_p [b]
Aqueous buffer	~370	~545	–
DMPC	~384[a]	~476[a]	8.39 ± 1.2
DMPG	~384[a]	~476[a]	5.34 ± 1.2

[a] [Lipid] = 2.0 mM.
[b] The partition coefficient (K_p) values are $\times 10^4$ order.

3. Results and discussions

3.1. Interaction of DPDAME with lipids: modulations of steady-state spectral properties

The absorption spectra of DPDAME (in buffer solution) in the presence of increasing concentration of lipids (DMPC and DMPG) is found to experience increment of absorbance with simultaneous little red shift of the maxima (refer Table 1). Such changes of the absorption spectral features can be realized in connection with a modified environment (such as change in micropolarity) in the immediate vicinity of the probe when present in the lipid environments, which in turn affects the stabilization of its different energy levels. With lowering of local polarity in the immediate vicinity of the fluorophore in lipid environments, the energy gap between HOMO (highest occupied molecular orbital) and LUMO (lowest unoccupied molecular orbital) decreases to give rise to the bathochromic shift. This is in consensus with reported literature also [2,3,11–14,16]. Furthermore, our interpretation is substantiated by a relative red shift of absorption maxima of DPDAME upon moving from aqueous solution to a non-polar medium like *n*-hexane or methylcyclohexane ($\lambda_{abs}^{max} \sim 370$ nm in water vs. $\lambda_{abs}^{max} \sim 375$ nm in *n*-hexane/methylcyclohexane) [34].

On the other side, emission spectral profile of DPDAME in aqueous buffer solution is found to undergo dramatic modifications as a result of interaction with DMPC or DMPG lipids. Fig. 2 illustrates the remarkable emission intensity enhancement coupled with an extensive shifting of the emission wavelength towards the blue[1] end of the spectrum with increasing lipid concentration (DMPC in Fig. 2a and DMPG in Fig. 2b).

Fig. 3 displays the marked modulations on the emission profile of the probe as a function of lipid concentration. An initial steep rise of intensity is found to be plateaued in the region of higher lipid concentration marking the saturation of the interaction. A direct comparison with the relative emission maxima positions of DPDAME in homogeneous solvents of varying polarity ($\lambda_{em} \sim 425$ nm in *n*-hexane vs. $\lambda_{em} \sim 476$ nm in tetrahydrofuran vs. $\lambda_{em} \sim 545$ nm in water i.e. medium polarity decrement accompanies blue shift [34]) makes way for realizing the observed spectral changes in terms of enhanced hydrophobicity in the immediate vicinity of the probe microenvironment within the liposomes as compared to aqueous buffer medium [16–23]. In fact, the magnitude of blue shift of the CT emission of DPDAME at a reasonable lipid concentration is quite astonishing: $\lambda_{em} \sim 545$ nm in aqueous buffer vs. $\lambda_{em} \sim 476$ nm in 2.0 mM DMPC/DMPG. The marked intensity enhancement of DPDAME can be rationalized in connection with restriction on rotational and vibrational degrees of freedom of the entrapped probe molecules within the lipids. A direct consequence of this will be rendered in depletion of radiationless decay channels with consequent emission intensity enhancement [7,11,14,16]. However, it could be too early to be precise on the location of the probe in the entire framework of the macromolecular system, the issue has been elaborated and substantiated in forthcoming discussions.

Here, the *anomalous* dual emission behaviour of the probe in aqueous medium and its subsequent modulation in lipid environments (*vide* Fig. 2) promoted us to make an attempt to resolve the emission spectra into individual Gaussian curves following the method described in the experimental section. Fig. 3c illustrates the deconvoluted fluorescence spectra of the probe DPDAME in representative environments as indicated in the figure legend. In bulk aqueous buffer medium the deconvolution into two individual Gaussian curves yields a simple picture in the sense that the resolved band components centred at $\lambda_1 = 442$ nm and $\lambda_2 = 556$ nm correspond to emission from the LE and the CT states of the probe, respectively. The deconvolution analysis for the fluorescence spectra of the lipid-bound probe was, however, not so simple. As seen in Fig. 3c, with increasing concentration of DMPC lipid the resolved Gaussian band component corresponding to the CT emission undergoes a gradual blue shift (from $\lambda_2 = 556$ nm in aqueous buffer to 503 nm in 0.15 mM DMPC and to 491 nm in 1.0 mM DMPC), in conformity to experimental findings. The resolved band component corresponding to the higher energy band in the experimental spectrum was found to be located at $\lambda_1 \sim 471$ nm in DMPC lipid and did not shift considerably as a function of lipid concentration. It is important to emphasize in the present context that the characteristics of the distinct components of DPDAME emission, particularly emission wavelength maximum and relative intensity will be governed by numerous factors including the polarity/viscosity of the probe microenvironment within the lipid, the extent of rotational motion of the probe in that environment, and so forth [35]. In fact, it also does not appear logical to assign the first component of the resolved band at $\lambda_1 \sim 471$ nm of lipid-bound DPDAME solely to the LE photo-excited state, rather a complicated modulation of the relative stability patterns of the LE and CT states appears to take place within the hydrophobic microheterogeneous lipid environments. Thus the deconvolution of the fluorescence spectrum of lipid-bound DPDAME into two individual Gaussian curves may be ascribed to the microheterogeneous environment in the immediate vicinity of its interaction site within the lipids or the presence of different ensembles of probe molecules varying in the degree of solvent-stabilization within the motionally constrained microheterogeneous environment of the lipids or an interplay of such factors [36]. The feasibility of the second aspect cannot be negated in the present context with an eye to the observation of wavelength-sensitive fluorescence parameter as discussed in a forthcoming Section 3.4. Therefore, the deconvolution of the fluorescence spectra into two Gaussian curves seem to reflect the simultaneous operation of several factors governing the average microenvironment in the immediate vicinity of the probe within its interaction site in the lipid. However, assignment of specific mechanistic model to each of the deconvoluted band is suppressed here as it could be misleading in the present context given the complex nature of the overall interaction. Similar results are also obtained in DMPG lipid but not mentioned here for the sake of conciseness.

[1] For interpretation of color in Fig. 2, the reader is referred to the web version of this article.

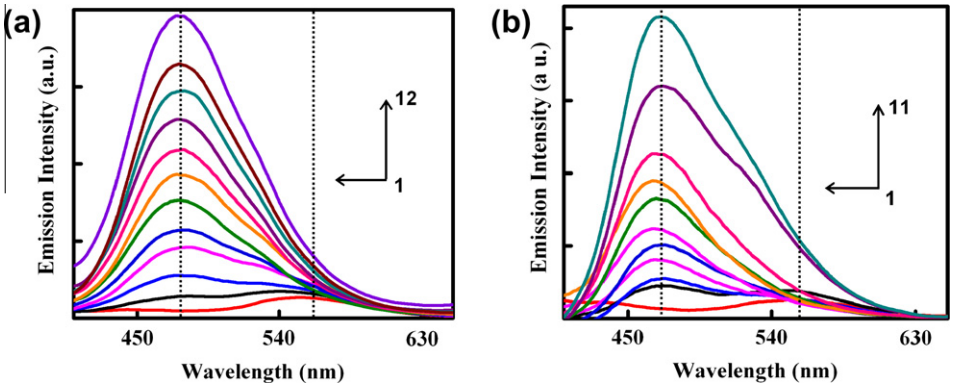

Fig. 2. Emission spectra (λ_{ex} = 370 nm) of DPDAME in the presence of increasing concentration of (a) DMPC (Curves 1 → 12 correspond to [DMPC] = 0.0, 0.02, 0.05, 0.09, 0.15, 0.30, 0.50, 0.70, 0.80, 0.90, 1.50, 2.00 mM) and (b) DMPG (Curves 1 → 11 correspond to [DMPG] = 0.0, 0.02, 0.05, 0.09, 0.30, 0.50, 0.70, 0.80, 0.90, 1.50, 2.00 mM). (For interpretation to colours in this figure, the reader is referred to the web version of this paper.)

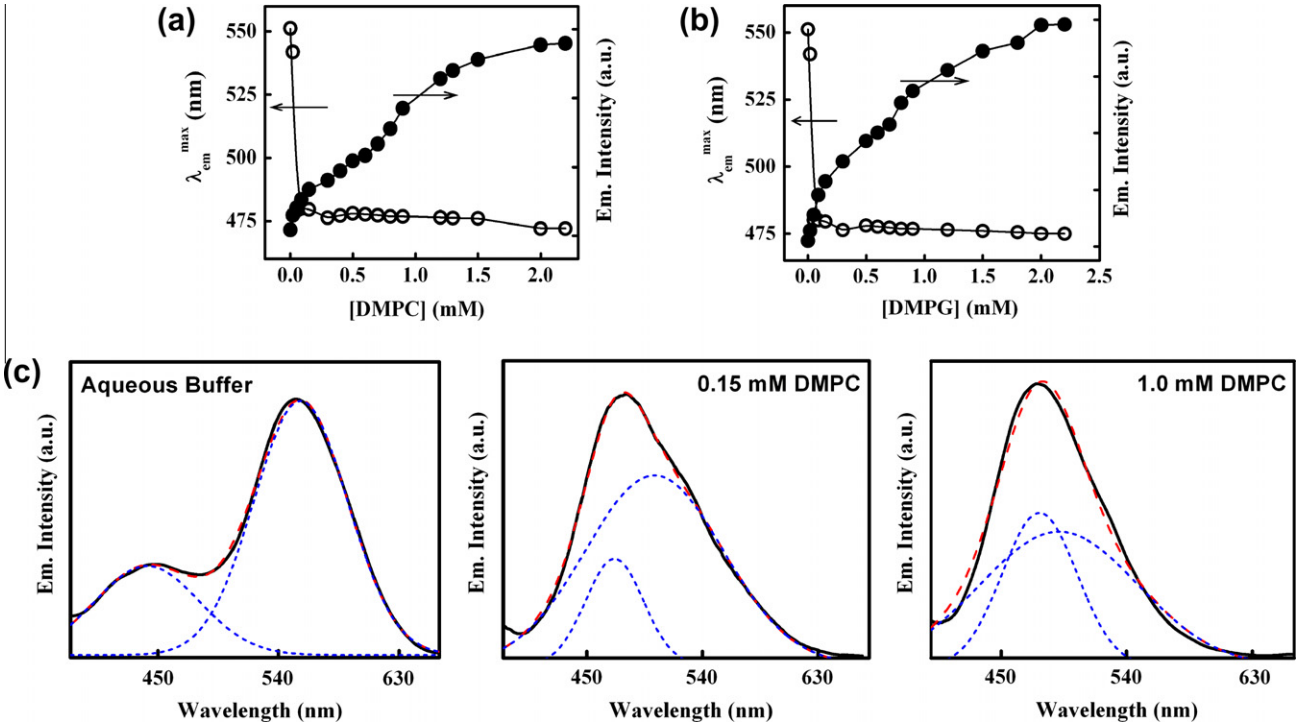

Fig. 3. Plot of simultaneous variation of emission intensity (-●-) and λ_{em}^{max} (nm) (-○-) of DPDAME as a function of lipid concentration: for (a) DMPC and (b) DMPG. The solid line is not a fitted line and only provides a visual guide to the pattern of variation. (c) Deconvolution of the emission spectra of DPDAME into two Gaussian curves in representative environments as indicated in the figure legend. The bold black lines designate the experimental spectra, blue dotted lines designate the resolved bands and the red dashed lines designate the convoluted spectra from the resolved bands. (For interpretation of the references to colour in this figure legend, the reader is referred to the web version of this article.)

3.2. Partitioning of the probe

A quantitative estimate of the extent of penetration of the probe into the lipid bilayer is obtained from the knowledge of partitioning of the probe between the lipid environments and aqueous phase. Since the partitioning of the probe is a function of the physical state and fluidity of the liposome membrane, quantitative determination of the partition coefficient will throw light into the extent as well as mechanism of access of the probe into the system. The partition coefficient (K_p) of the probe between the liposomal phase and aqueous phase is given by the following relation, as defined by Rodrigues et al. [41]

$$K_p = \frac{(C_m/C_t)/[\text{Lipid}]}{(C_w/C_t)/[\text{Water}]} \tag{6}$$

where C_t is the total molar concentration of probe, C_m and C_w stand for probes in lipid (DMPC/DMPG) and in water (aqueous buffer), respectively. Terms within square brackets represent molar concentration of respective species. The evaluation of partition coefficient of DPDAME rests on an analysis of the fluorescence data according to the following equation [16,41,42]:

$$\frac{I_\infty - I_0}{I_x - I_0} = 1 + \frac{[\text{Water}]}{K_p} \times \frac{1}{[\text{Lipid}]} \tag{7}$$

in which I_0, I_x and I_∞ stand for fluorescence intensities of the probe DPDAME in the absence, at an intermediate and at saturation level of lipid concentration, respectively. From the plot of $(I_\infty - I_0)/(I_x - I_0)$ vs. $[\text{Lipid}]^{-1}$ the partition coefficient values are calculated: $K_p = (8.39 \pm 1.2) \times 10^4$ in DMPC and $(5.34 \pm 1.2) \times 10^4$ in DMPG

lipid. Such high magnitude of K_p is, indeed, a clear manifestation of efficient partitioning of the probe in liposome membrane. Also the present findings corroborate well to previous reports [16–22,42,43].

A summary of the binding interaction of DPDAME with the studied lipid systems is collected in Table 1. It is interesting to note the comparable magnitudes of K_p in both the lipid environments. This observation could be treated as a manifestation of equivalent sort of interaction of the extrinsic probe DPDAME with both the liposome membranes, which in turn tends to substantiate our observations on steady-state emission spectral studies (Section 3.1 and Figs. 2 and 3).

The results discussed in the foregoing sections display the spectroscopic monitoring of the interaction of DPDAME with the studied lipids. The polarity-dependent ICT emission of the probe exhibits discernible sensitivity to the microheterogeneous environments of lipids in terms of remarkable emission intensity enhancement coupled with a large spectral blue shift. It is thus quite naturally pertinent to explore the binding site of the probe within the complex lipid environments so as to follow the site-specific efficacy of the probe to function as a molecular reporter. In order to assess the binding site, we have pursued the following arguments.

Initial insights about the location of the probe into hydrophobic tail part of the lipid were derived from steady-state emission spectral modulations induced by increasing concentration of the lipids (Figs. 2 and 3). It was, indeed, surprising to note that the presence of both the lipids DMPC and DMPG ensures quite analogous modification to the emission characteristics of DPDAME (with all experimental conditions conserved) signalling towards the environment of the probe being equivalent in both the lipids. This observation is rationalized based on the idea of incorporation of DPDAME into hydrophobic interior of DMPC and DMPG lipids. As for otherwise, had the probe been located in the head-group region, similar spectral features could have not been expected in the presence of DMPC and DMPG as because of their differential surface charges (DMPG head-group is anionic while DMPC head-group is zwitterionic). Differential electrostatic interactions with the surface charges of the lipid head-groups should have been manifested in remarkably polarity-sensitive ICT emission profile of DPDAME [34]. This postulation is further substantiated through quantitative perusal of emission data in terms of elucidation of partition coefficient which reveals comparable magnitudes in both cases.

Fluorescence quenching experiments performed with bare DPDAME (in Tris–HCl buffer) and lipid-bound DPDAME proved to be a fruitful technique to provide added support in assessing the location of the probe inside the lipid bilayer. This strategy has been extensively utilized [11,14] to locate an external fluorophore in a biological or biomimicking assembly. The concept of the work relies on some simple modulations of electrostatic interactions between the probe and an ionic quencher (here Ni^{2+}). A transition metal cation (Ni^{2+}) is expected to quench the fluorescence of a bare fluorophore (DPDAME) on account of its usual quenching actions as depicted in Fig. 4 (the quenching of fluorescence intensity is followed on Stern–Volmer equation i.e. $I_0/I = 1 + K_{SV}[Q]$ [7]. Here I_0 is the original fluorescence intensity, I is the quenched intensity and [Q] is the molar concentration of the quencher Q (here Ni^{2+}). The Stern–Volmer quenching constant K_{SV} yields a measure of the extent of interaction between the fluorophore and the quencher. The higher the magnitude of K_{SV}, the more efficient is the quenching ensuring the greater is the degree of exposure of the quencher to the probe.). On performing the same quenching experiment, under conditions of all experimental factors/instrument settings conserved, on lipid-bound DPDAME, the extent of quenching is expected to be improved with DMPG if the probe is located in its head-group region [11,14,16]. Favourable (attractive) electrostatic

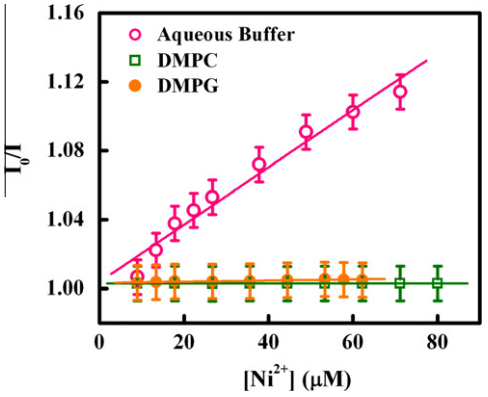

Fig. 4. Stern–Volmer plot for Ni^{2+} ion-induced quenching of fluorescence of DPDAME in aqueous buffer medium and in the presence of lipids ([Lipid] = 1.0 mM in each case). Respective environments are specified in the figure legend.

affair between the surface charges of DMPG (negative) and the quencher (positive) should ensure a closer approach of the quencher to the fluorophore resulting in enhanced fluorescence quenching. Whereas Fig. 4 displays some contrasting results, i.e. Ni^{2+} is able to induce almost no quenching of lipid-bound probe be it DMPC or DMPG, relative to that for bare fluorophore (DPDAME in Tris–HCl buffer). This result receives a sound interpretation on grounds of penetration of the probe to the hydrophobic tail part of the lipid which will subsequently negate the penetration of a charged species (Ni^{2+}) whereby confirming a feeble interaction between the quencher and the fluorophore.

3.3. Steady-state fluorescence anisotropy

Steady-state fluorescence anisotropy (r) study is central to biochemical and biophysical research owing to its commendable ability to produce valuable information about the environments in the immediate vicinity of the fluorophore. The microenvironment of the probe molecule is governed by its precise location in complex molecular assembly. Any modulation in the rigidity of the surrounding environment of the fluorophore will be reflected through anisotropy values. The so-called environment induced motional restriction on the mobility of the probe in biological membranes is manifested through anisotropy variation and thereby furnishing clues to assay the location of the probe within the complex biological environments [7,14,16,19,20,32,43]. In the present case, the fluorescence anisotropy of DPDAME (Fig. 5a) exhibits specific variation as a function of the lipid concentration. An initial steep rise in the anisotropy value indicates increasing degree of motional restriction on the probe imparted by the confined environment of lipid bilayers up to lipid concentration of 0.8–1.0 mM followed by attainment of a plateau region marking the saturation of interaction between the two parties. Interestingly, the concentration of DMPC or DMPG (0.8–1.0 mM) at which the plateau region starts showing its onset is strikingly corresponding to that obtained from emission intensity data (*vide* Fig. 3). Thus the steady-state anisotropy measurements seem to strongly complement the emission spectral data and the inferences drawn therefrom [7,19,20,32,43–49].

Furthermore, a significant increase in anisotropy as a function of the excitation wavelength is observed for DPDAME in lipid environments. Fig. 4b displays the excitation anisotropy profile for various concentrations of lipids. This effect is attributed to the slow rate of solvent reorientation around the fluorophore in the excited state in organized media and hints towards location of the probe in motionally constrained environments [7,44–46,50,51]. This

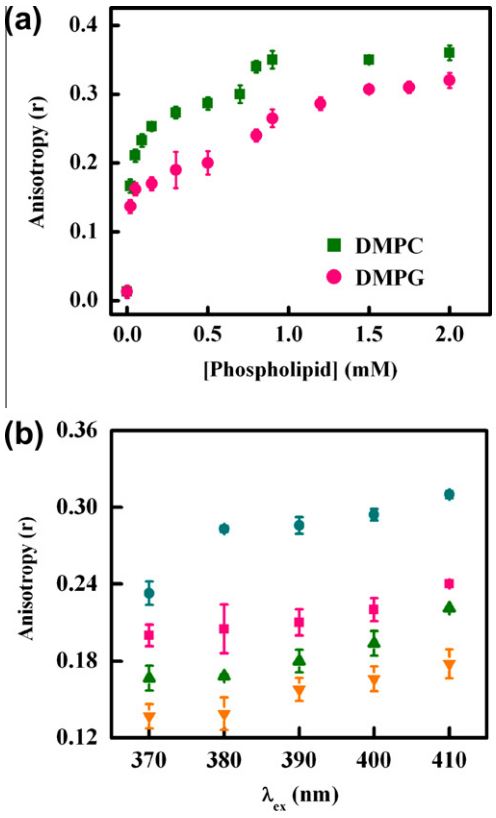

Fig. 5. (a) Variation of steady-state fluorescence anisotropy (r) of DPDAME (λ_{ex} = 370 nm and $\lambda_{monitored} = \lambda_{em}^{max}$) with increasing concentration of lipid in DMPC and DMPG environments. (b) Representative excitation anisotropy profile (variation of steady-state fluorescence anisotropy as a function of excitation wavelength) for DPDAME at some defined lipid concentrations, e.g., 0.02 mM (-▲-) and 0.15 mM (-●-) DMPC and 0.2 mM (-▼-) and 0.8 mM (-■-) DMPG. Each anisotropy data point is an average of 20 individual measurements under same experimental condition. Error bars are within the symbols if not apparent.

observation has been more elaborately addressed in corroboration to red-edge excitation shift study in the forthcoming section.

3.4. Wavelength-selective fluorescence parameter: the red-edge excitation effect

The Red Edge Excitation Shift (REES) is a set of wavelength sensitive tools for directly monitoring the solvation dynamics within an organized medium. REES in organized assemblies arises primarily out of the spatial heterogeneity of these assemblies. This consists of multiple solvation sites and contribute to inhomogeneous broadening of the absorption spectra [12,27,44–46], which in turn allows the provision of site photoselection. The excitation wavelength dependence can, however, arise when there exists ensemble of molecules in the ground state which differ in their solvation sites and, hence, their energies. Though achievement of this condition alone does not ascertain the occurrence of REES due to rapid relaxation of the excited state in form of rapid solvation of the fluorescent state or energy transfer between close-lying excited states or different conformers. Precisely, the operation of REES is subject to the following conditions:

(a) The molecule should be polar with dipole moment higher in the excited state than that in the ground state. In fact, the extent of inhomogeneous broadening of the absorption spectra allowing the provision of site photoselection of energetically different species is dependent on the change of dipole moment ($\Delta\mu$) following photoexcitation through the relation $\Delta\upsilon = A\Delta\mu\rho^{-3/2}\ (kT)^{1/2}$ according to Onsager sphere approximation [44] (here A is a constant that depends on the dielectric constant of the medium and ρ is the Onsager cavity radius). Solvatochromic measurements evidence a marked increase of dipole moment of DPDAME upon photoexcitation to the excited singlet state: μ_{ES} = 20.06 D vs. μ_{GS} = 3.64 D i.e. ($\Delta\mu$ = 16.42 D as calculated using Lippert–Mataga equation with μ_{GS} = 3.64 D as obtained from DFT//B3LYP/6-31G (d,p) level of calculation [34]). However, additional broadening, which can play even a greater role in inhomogeneous broadening of absorption spectra, may be induced by specific interactions of the sort of hydrogen bonding, electrostatic interactions and so forth [44–46,50–52].

(b) The solvent molecules around the fluorophore must be polar and the solvent reorientation time ($\langle\tau_{solvent}\rangle$) should be slower or comparable to the fluorescence life-time (τ_f) of the fluorophore so that unrelaxed fluorescence can give rise to excitation-wavelength-dependent emission behaviour. Thus the phenomenon of REES provides a more vivid picture of the surrounding atmosphere of the fluorophore while emitting from the excited state.

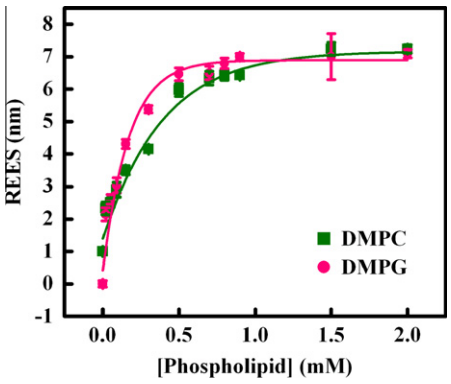

Fig. 6. Plot of REES (nm) (due to change of λ_{ex} from 370 nm to 430 nm) vs. [Lipid] (mM) in DMPC and DMPG environments. Error bars are within the marker symbols if not apparent.

Fig. 6 reflects the occurrence of REES in the present system of investigation. The magnitude of REES increases with lipid concentration to 7.24 nm in 2.0 mM DMPC and 7.10 nm in 2.0 mM DMPG. This observation, therefore, suggests that binding of the probe to lipids imparts restriction to the reorientation of solvent dipoles around the excited fluorophore. Furthermore, specific interactions is not unlikely to contribute to the operation of REES through additional broadening of absorption spectra (as mentioned above) [44,46]. REES measurements have been performed with intense care to ensure that the change of excitation wavelength involves shifting of λ_{ex} to the red end of the absorption spectra and not merely the absorption maxima [44–46]. Excitation wavelength has been varied from 370 nm (λ_{abs}^{max}) to 430 nm. For λ_{ex} beyond 430 nm, observations were obscured by significant lowering of signal-to-noise ratio, appreciable broadening of emission spectra and contamination from artifacts due to Rayleigh peaks which persisted even after background correction.

3.5. Micropolarity around the fluorophore

The precise determination of the microscopic polarity of biological and biomimicking assemblies is an important goal in biological and biochemical research. Any method possessing a healthy balance between its accuracy and cost-effectiveness in this perspective is thus always appreciated. Environment sensitive fluorescent probes have been recognized for serving the purpose since a couple

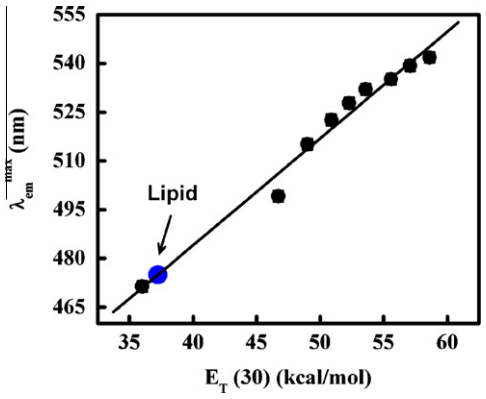

Fig. 7. Plot of variation of emission maxima of DPDAME with polarity equivalent parameter $E_T(30)$ (kcal/mol) in different compositions of dioxane-water mixture. The polarity of the DPDAME binding site in liposome environment is indicated on the calibration curve. [Lipid] = 2.0 mM. Error bars are within the marker symbols if not apparent.

of decades [11,12,14,16,24]. Local polarity of the biomimetic environment like liposome membrane can be estimated by comparing the spectral properties of the fluorophore in the environment with those in pure solvent or solvent mixture of known polarity. Although the polarity of a microheterogeneous environment is not exactly the same as that of a homogeneous fluid, a relative estimate of the micropolarity around the fluorophore generally yields reliable results [11,12,14,16,24]. In this section we demonstrate the utilization of medium polarity-dependent emission behaviour of DPDAME to estimate the micropolarity of its immediate surroundings in the lipid environments. In Fig. 7, a calibration curve has been constructed by plotting the emission maxima of DPDAME in different compositions of water–dioxane mixtures of known polarity as a function of polarity equivalent parameter, $E_T(30)$ [53]. Interpolation of the numerical magnitude of the emission maxima of the probe when bound to 2.0 mM DMPC or DMPG on the linear regression leads to a polarity value of 37.24 on $E_T(30)$ scale for the microheterogeneous system. Thus in lipid bilayer, the polarity of the immediate vicinity of the probe matches reasonably well to that of tetrahydrofuran ($E_T(30)$ (kcal/mol) = 37.4 [53]; the λ_{em}^{max} of DPDAME in tetrahydrofuran (~476 nm) [34] is close to that in the presence of the lipids). Therefore, a marked lowering of polarity surrounding the probe in the presence of DMPC or DMPG membrane (relative to that in bulk aqueous phase, $E_T(30)$ (kcal/mol) = 63.1 [53]) strongly implies location of the probe in the hydrophobic tail part of the lipid systems. That the micropolarity around the extrinsic probe amounts to $E_T(30)$ (kcal/mol) = 37.24 in both DMPC and DMPG suggests that the average environment surrounding the probe is equivalent in both the lipids. Had the polarity-sensitive probe been located in the head-group of the lipids, micropolarity in its immediate vicinity should have certainly been different in the two cases [16,28]. Furthermore, an $E_T(30)$ value of 37.24 closely resemble the polarity of hydrophobic tail region of the lipid bearing excellent consistency with literature report. A recent report by Cohen et al. [54] demonstrated the construction of NMR-based molecular ruler for determining the depth of intercalants within lipid bilayer. In direct analogy with their report we estimate that the polarity of $E_T(30)$ (kcal/mol) = 37.24 (i.e. within 34–44) corresponds to penetration of DPDAME around 7.4–16.4 Å deep into the bilayer [54].

3.6. Dynamical aspects of probe–lipid interaction

3.6.1. Fluorescence decay study

By virtue of its sensitivity to the environments and excited state interactions, fluorescence lifetime serves as an indicator to explore the environment around a fluorophore. It also furnishes valuable information regarding binding of a probe with lipids [2,3,7,11–16,55]. Fig. 8 illustrates the typical time-resolved fluorescence decay profiles of the probe DPDAME in various environments indicated in the figure legends and the corresponding fitting parameters are collected in Table 2. In view of the complicated functional and structural architecture of lipid membranes it is not surprising to have mutiexponential decay profiles of DPDAME in the presence of DMPC and DMPG lipids. Thus without putting much emphasis on the individual decay time constants we chose to employ the mean (average) fluorescence lifetime as an important tool to exploit the behaviour of DPDAME in the presence of lipids [7,11,14,16,32]. In fact, the data compiled in Table 2 unveils that the microenvironment around the probe is enormously modified in the presence of the lipids whereby emphasizing the selection of average lifetime for extraction of meaningful results.

In analogy to literature reports [7,11,14–16,20,32,47], and modulations of excited state photophysics of the probe in proteineous and micellar environments [33], the increase of lifetime associated with increasing lipid concentration (Table 2) seems attributable to depletion of nonradiative decay channels through reduction of rotational/vibrational degrees of freedom resulting from its encapsulated state in lipid microheterogeneous environments. In order to further interpret the modulations in excited state behaviour of DPDAME we have calculated the radiative (k_r) and nonradiative (k_{nr}) decay rate constants (Table 2) using the following two equations [7,33]:

$$k_r = \frac{\Phi_f}{\langle \tau_f \rangle} \tag{8}$$

$$k_{nr} = \frac{1}{\langle \tau_f \rangle} - k_r \tag{9}$$

Here, Φ_f is the fluorescence quantum efficiency and $\langle \tau_f \rangle$ is the average fluorescence lifetime calculated from Eq. (3). Scrutiny of the data in Table 2 reveals that the radiationless decay rates are considerably reduced in lipid environments compared to that in bulk aqueous buffer medium whereby substantiating our previous arguments. Furthermore, that the fluorescence quantum efficiency (Φ_f), and mean lifetime ($\langle \tau_f \rangle$) of the probe appears comparable at a defined concentration of either of the lipids (DMPC and DMPG; *vide* Table 2) seems to corroborate, in consensus with the steady-state emission spectra (*vide* Fig. 2), to the postulation that the average environment in immediate vicinity of the probe is identical in both the studied lipids.

Further, it is interesting to note the nature of modulation of time-resolved fluorescence decay patterns of the probe in lipid environments. However, an unequivocal interpretation for the biexponential decay behaviour of the probe in bulk aqueous buffer medium is yet to be realized. The data compiled in Table 2 reveals a significant modification of the fluorescence decay behaviour of DPDAME in the studied lipid environments yielding a major contribution from a short-lived ($\tau_3 \sim 1$ ns) component. In spite of the difficulties in assigning specific mechanistic models to the individual decay components, as pointed out by many workers [7,11,14,16,32], we endeavour to look into the interaction scenario on the basis of a comparison with fluorescence decay properties of the probe in homogeneous solvents. The discussion in Section 3.5 reveals that the micropolarity in the immediate vicinity of the probe within the lipids ($E_T(30)$ (kcal/mol) ~ 37.24) closely resembles with that of tetrahydrofuran ($E_T(30)$ (kcal/mol) = 37.4 [53]). Thus obviously, a proper comparative assessment for the fluorescence decay behaviour of the probe within the lipids could be drawn from fluorescence lifetime of DPDAME in tetrahydrofuran. Unfortunately the fluorescence lifetime of the probe in

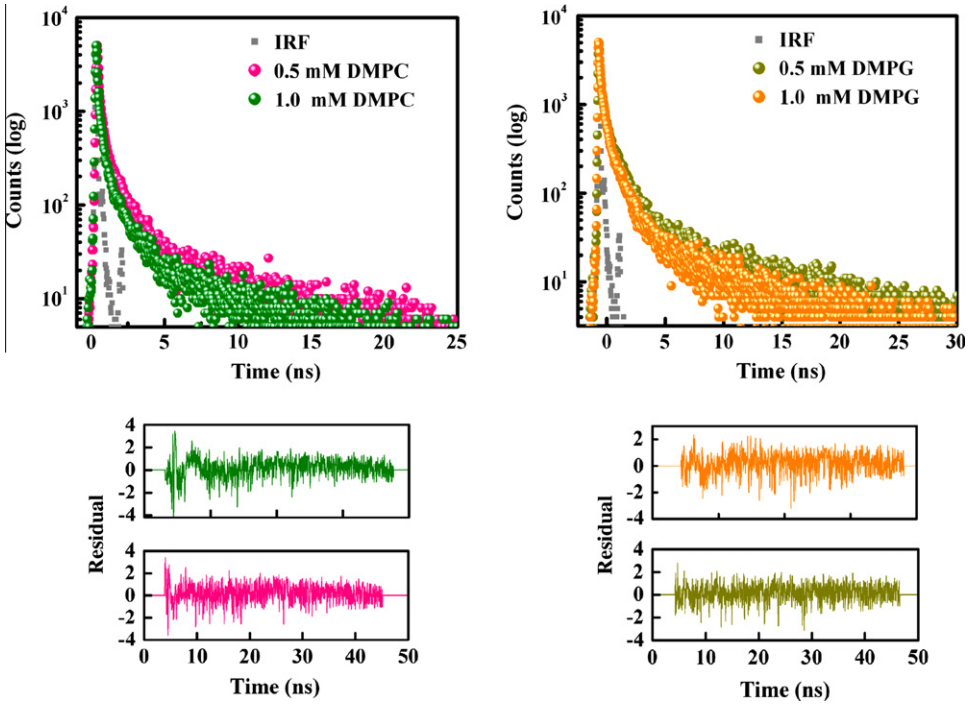

Fig. 8. Typical time-resolved fluorescence decay profiles of DPDAME in different environments as specified in the figure legends (λ_{ex} = 370 nm and $\lambda_{monitored} = \lambda_{em}^{max}$). The lower panel shows the residual plot for the respective fitted functions to actual data.

Table 2
Time-resolved fluorescence decay parameters, quantum yield (Φ_f), radiative (k_r) and non-radiative (k_{nr}) decay rate constants of DPDAME in lipids.

Environment	τ_1/ns (α_1)	τ_2/ns (α_2)	τ_3/ns (α_3)	$\langle\tau_f\rangle$/ns	χ^2	Φ_f	$k_r \times 10^{-7}$ (s^{-1})	$k_{nr} \times 10^{-9}$ (s^{-1})
Aqueous buffer	0.508 (0.934)	1.696 (0.065)	–	0.732	0.98	0.034	4.64	1.32
0.5 mM DMPC	0.903 (0.053)	7.13 (0.003)	0.092 (0.944)	1.305	1.11	0.076	5.82	0.71
1.0 mM DMPC	0.814 (0.081)	6.741 (0.005)	0.079 (0.914)	1.581	1.19	0.098	6.2	0.57
0.5 mM DMPG	0.914 (0.064)	7.3 (0.003)	0.097 (0.93)	1.302	1.27	0.081	6.22	0.71
1.0 mM DMPG	1.124 (0.223)	7.88 (0.009)	0.152 (0.77)	1.956	1.19	0.11	5.62	0.46

tetrahydrofuran was too fast to detect within the measuring limit of our instrument [34]. Thus it is argued that the impartation of motional restrictions on the probe molecules within its encapsulated state in the lipids results in reduction of nonradiative decay channels and hence enhances fluorescence lifetime (*vide* Table 2). It is probable that the short-lived major component in the fluorescence decay of DPDAME in lipids actually reflects the average local environment in the immediate surroundings of the lipid-bound probe molecules. However, the issue of considerable heterogeneity in the overall fluorescence decay behaviour of the lipid-bound probe in terms of multiexponential decay pattern (Table 2) remains a point to be noted. Such superposition of many decays of different lifetimes leading to an overall multiexponential decay is quite common for a polarity sensitive probe molecule and has been discussed by many workers [7,11,14,16,32]. Obviously extraction of meaningful rate constants in such heterogeneous systems is really difficult. As pointed out by Robinson et al. [56], if the diffusion coefficient of the probe in the microheterogeneous environment is the same as that in bulk water, the probe may undergo excursion over a region of radius ~1 nm/ns within its lifetime in a direction normal to the surface and may experience different environments. Even if we assume that within the lipid microheterogeneous environment the diffusion or excursion is rather slow, the possibility of heterogeneity in the overall fluorescence decay behaviour of the probe giving rise to multiexponential decay pattern cannot be ruled out given the possibilities of unequal hydration for the probe containing so many heteroatoms. In fact, a justification for such possibility may be argued in connection with the observation of wavelength-sensitive fluorescence properties of the probe within the microheterogeneous lipid environments (*vide* Section 3.4), since this may be a contributing factor in allowing site selective photoexcitation of the lipid-bound probe molecules leading to the operation of REES (*vide* Fig. 6) [44–46].

3.6.2. Rotational relaxation dynamics: time-resolved fluorescence anisotropy decay

The time-dependent decay of fluorescence anisotropy is a sensitive indicator of the rotational motion and/or rotational relaxation of the fluorophore in an organized assembly [7,14,16,57]. Therefore, with a view to delve into the microenvironment in the immediate vicinity of lipid bound-DPDAME, time-resolved fluorescence anisotropy decay has been recorded as a function of lipid concentration. The representative anisotropy decay profile is displayed in Fig. 9 and the relevant dynamic parameters are summarized in Table 3. The rotational relaxation time for the free probe (DPDAME in aqueous buffer phase) was too fast to allow extraction

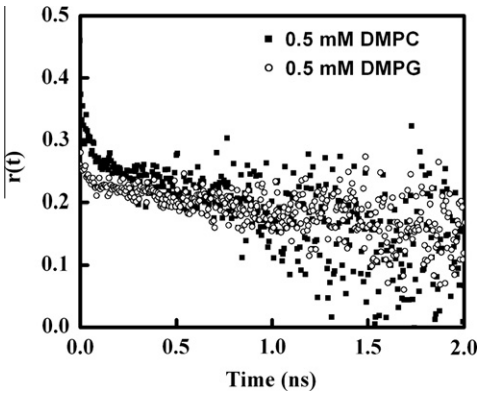

Fig. 9. Representative time-resolved anisotropy decay profile for DPDAME in DMPC and DMPG lipids (λ_{ex} = 370 nm and $\lambda_{monitored} = \lambda_{em}^{max}$).

Table 3
Time-resolved fluorescence anisotropy decay parameters of DPDAME in lipid environments.

Environment	Relative amplitude (%)	τ_r (ns)	χ^2
0.5 mM DMPC	100	1.08	1.2
1.0 mM DMPC	100	1.6	1.18
0.5 mM DMPG	100	1.09	1.21
1.0 mM DMPG	100	1.84	1.18

of reliable decay parameter within our instrumental (typical instrument time resolution ~ 80 ps). However, a notable enhancement of the rotational relaxation time of the probe in lipids (Table 3) confirmed the signature for impartation of considerable degree of rigidity in the microenvironment of the probe within the lipids.

A single exponential decay function has been exploited to adequately describe the anisotropy decays of DPDAME in both the lipids (Table 3) [7,14,16]. Now, several arguments might emanate to account for the relaxation of the fluorescence anisotropy of the probe in liposomal phase. The following possibilities are thus taken into consideration [7,11,14,16]: (i) the fluorophore rotates within the lipid; (ii) the entrapped fluorophore cannot rotate but the liposome unit carrying the probe rotates; (iii) both rotations are possible.

The third option is immediately disqualified with a view to the observed single exponential anisotropy decay, since a biexponential decay pattern can only suitably interpret the possibility of both the rotations being operative. Now, in an endeavour to confirm one of the former two possibilities we have calculated the rotational relaxation times of the liposome units (τ_L) according to the Stokes–Einstein–Debye (SED) relation [7,14,16,57–59]:

$$\tau_L = \frac{4}{3}\pi r_h^3 \times \frac{\eta}{k_B T} \tag{10}$$

Here, η is the coefficient of viscosity of water, r_h is the hydrodynamic radius of the liposome units (as obtained from DLS measurement described in Section 2.3), k_B is the Boltzmann constant, T is the Kelvin temperature. That the rotational relaxation times of the liposome units are remarkably higher (data not shown) than the corresponding depolarization times of the fluorescence in the respective environments provides reasonable platform to believe that the relaxation of the fluorescence anisotropy is attributable to the rotation of the probe only and not of the liposome units [7,14,16,54,57–59].

Now, at this stage, it could be intriguing to opt for a critical assay of the time-resolved anisotropy decay parameters of DPDAME in both the lipids, and an endeavour along this line invites the following arguments. Firstly, the single exponential anisotropy decay pattern of the probe in lipid environments ensures absence of inhomogeneity in the rotational relaxation dynamics of DPDAME in the presence of lipids [7]. At the same time, it is worth noting that at a defined concentration of either of the lipids (DMPC or DMPG) the rotational relaxation time (τ_r) of the probe registers a comparable magnitude (Table 3). These observations, apart from corroborating to our previous findings, put their signature towards reinforcing the previous interpretation that the probe molecule experiences similar microenvironments in both the lipids. This, in turn, can be rationalized upon consideration of probable location of the probe to be in the hydrophobic interior of the liposome units and not in the head-group region which are endowed with differential surface charge characteristics.

4. Summary and conclusion

The present study reports the spectroscopically monitored binding interaction of the ICT probe DPDAME with two well-known lipid systems viz. DMPC and DMPG. The commendable sensitivity of the ICT emission property of the probe towards medium polarity has been exploited to successfully report the micropolarity of the site of interaction of DPDAME within the lipids. The micorpolarity measurement in juxtaposition with other experimental findings (e.g., red-edge excitation, ionic quencher (Ni^{2+}-ion)-induced steady-state fluorescence quenching, and time-resolved studies), advocates for probable location of the probe to be in the hydrophobic interior of the liposome membranes. Time-dependent anisotropy study reflects the impartation of motional restriction on the probe within the lipids.

While many fluorophores are reported to be located in the lipid head-group region, DPDAME is a prospective candidate in probing the microheterogeneous environments of the hydrophobic interior of the liposomes. The medium polarity-sensitive ICT emission of DPDAME appears to provide additional technical edges to the probe in serving as a molecular reporter for the said purpose. Further, it is worthwhile to note that the significant enhancement of dipole moment of DPDAME following photo-excitation is an important prerequisite for the probe for sensing of the spatial heterogeneity of the microheterogeneous liposomal assemblies leading to the occurrence of REES, which in turn allows the monitoring of solvent-relaxation around the excited fluorophore (as discussed in Section 3.4). It is to note in the present context that the model membrane probe DPH also did not exhibit REES in lipid environments [60]. Since the hydrophobic core of the lipid bilayer is comprised of methylene and methyl groups in DMPC and DMPG lipids, the only solvent dipoles capable of interaction with the excited dipole of the fluorophore leading to the operation of REES have to be the water molecules that have penetrated deep into the bilayer close to the location of the probe. The observation thus addresses an important issue, that of whether water penetration occurs in the inner hydrophobic region of the lipid bilayers. Convincing reports demonstrating the presence of water in the deeper hydrocarbon region of the membrane are rather only sporadically addressed in the literature [61]. The present results thus suggest the occurrence of water penetration in the deeper regions of the lipids (at least under the present experimental conditions), and is also consistent with a recent report [62]. The nature of rotational relaxation in the hydrophobic interior of the lipids is also probed by DPDAME fluorescence.

In fact, the location of the extrinsic probe in the hydrophobic interior of the lipids coupled with its environment-sensitive photophysics have triggered its further applications in monitoring of important phenomena e.g., membrane fusion, disruption (solubilization) of lipid bilayers in surfactants and so forth [63] (works

underway in our laboratory). However, here we do not mention a detailed account of these results given the aim and scope of the present work.

Overall, we have demonstrated the potential of the self-designed ICT probe to function as a molecular reporter for microheterogeneous environments of liposome membranes under easy to moderate experimental conditions. With a view to the simplicity of the presently employed experimental techniques and efficiency of the extrinsic molecular reporter, we are optimistic that its applicability will leave ample scope for viable expansion of the field.

Acknowledgments

B.K.P. acknowledges C.S.I.R., India for research fellowship. N.G. acknowledges D.S.T. (Project no. SR/S1/PC/26/2008), Government of India for financial support. The authors appreciate the technical cooperation received from Ms. A. Gayen and Prof. C. Mukhopadhyay of Department of Chemistry of our University during preparation of the liposomes. The authors convey their special thanks to Prof. K.P. Das and Mr. P. Dey of Bose Institute, India for allowing us to use their DLS instrument. We also gratefully acknowledge the instrumental facilities of Indian Association for the Cultivation of Science, India and Mr. R. Pramanik, Prof. N. Sarkar of Indian Institute of Technology-Kharagpur, India for time-resolved studies.

References

[1] E. Lippert, W. Rettig, V. Bonacic-Koutecky, F. Heisel, J.A. Mieche, in: I. Prigogine, S.A. Rice (Eds.), Advances in Chemical Physics, vol. 68, Wiley-Interscience, New York, 1987, pp. 1–173 and references therein.
[2] A. Chakraborty, S. Kar, D.N. Nath, N. Guchhait, J. Phys. Chem. A 110 (2006) 12089–12095.
[3] S. Mahanta, R.B. Singh, S. Kar, N. Guchhait, J. Photochem. Photobiol. A: Chem. 194 (2008) 318–326.
[4] H. Ishikawa, Y. Shimanuki, M. Sugiyama, Y. Tajima, M. Kira, N. Mikami, J. Am. Chem. Soc. 124 (2002) 6220–6230.
[5] J.-S. Yang, K.-L. Liau, C.-M. Wang, C.-Y. Hwang, J. Am. Chem. Soc. 126 (2004) 12325–12335.
[6] I. Gomez, M. Reguero, M. Boggio-Pasqua, M.A. Robb, J. Am. Chem. Soc. 127 (2005) 7119–7129.
[7] J.R. Lakowicz, Principles of Fluorescence Spectroscopy, Plenum, New York, 1999.
[8] Z.R. Grabowski, K. Rotkiewicz, W. Rettig, Chem. Rev. 103 (2003) 3899–4032.
[9] E. Lippert, W. Luder, F. Moll, W. Nagele, H. Boos, H. Prigge, L. Seibold-Blankenstein, Angew. Chem. 73 (1961) 695–706.
[10] J.R. Durrant, S.A. Haque, E. Palomares, Chem. Commun. (2006) 3279–3289. and references therein.
[11] A. Mallick, B. Haldar, N. Chattopadhyay, J. Phys. Chem. B 109 (2005) 14683–14690.
[12] R.B. Singh, S. Mahanta, A. Bagchi, N. Guchhait, Photochem. Photobiol. Sci. 8 (2009) 101–110.
[13] M. Novaira, F. Moyano, M.A. Iasutti, J.J. Silber, N.M. Correa, Langmuir 24 (2008) 4637–4646. and references therein.
[14] R.B. Singh, S. Mahanta, N. Guchhait, Spectrochim. Acta 72 (2009) 1103–1111. and references therein.
[15] A. Chakraborty, N. Guchhait, J. Inclusion, Phenom. Macrocyclic Chem. 62 (2003) 91–97.
[16] B.K. Paul, N. Guchhait, J. Phys. Chem. B 114 (2010) 12528–12540. and references therein.
[17] J. Sujatha, A.K. Mishra, Langmuir 14 (1998) 2256–2262.
[18] M. Mohapatra, U. Subuddhi, A.K. Mishra, Photochem. Photobiol. Sci. 8 (2008) 1373–1378.
[19] C.R. Mateo, A. Douhal, Proc. Natl. Acad. Sci. USA 95 (1998) 7245–7250.
[20] S. Chaudhuri, B. Pahari, P.K. Sengupta, Biophys. Chem. 139 (2009) 29–36.
[21] R. Das, A.S. Klymchenko, G. Duportail, Y. Mely, J. Phys. Chem. B 112 (2008) 11929–11935. and references therein.
[22] M. Kozak, L. Domka, S. Jurga, J. Mol. Struct. 846 (2007) 108–111. and references therein.
[23] P.M. Nassar, L.E. Almedia, M. Tabak, Langmuir 14 (1998) 6811–6817.
[24] D. Marsh, Proc. Natl. Acad. Sci. USA 98 (2001) 7777–7782.
[25] B.N. Olsen, P.H. Schlesinger, N.A. Baker, J. Am. Chem. Soc. 131 (2009) 4854–4865.
[26] J.D. Perlmutter, J.N. Sachs, Biochim. Biophys. Acta 1788 (2009) 2284–2290.
[27] A. Ottova, H.T. Tien, Bioelectrochemistry 56 (2002) 171–173.
[28] J. Voskuhl, B.J. Ravoo, Chem. Soc. Rev. 38 (2008) 495–505.
[29] K. Kachel, E. Asuncion-Punzalan, E. London, Biochim. Biophys. Acta 1374 (1998) 63–76.
[30] N.M. Correa, H. Zhang, Z.A. Schelly, J. Am. Chem. Soc. 122 (2000) 6432–6434.
[31] N. Ashgarian, Z.A. Schelly, Biochim. Biophys. Acta 1418 (1999) 295–306.
[32] D.D. Lasic, Liposomes: From Physics to Application, Elsevier, Amsterdam, 1993.
[33] B.K. Paul, A. Samanta, N. Guchhait, J. Phys. Chem. B 114 (2010) 6183–6196.
[34] B.K. Paul, A. Samanta, S. Kar, N. Guchhait, J. Lumin. 130 (2010) 1258–1267.
[35] K.K. Karukstis, L.A. Perelman, W.K. Wong, Langmuir 18 (2002) 10363–10371. and references therein.
[36] E.A. Lissi, E.B. Abuin, M.A. Rubio, A. Ceron, Langmuir 16 (2000) 178–181. and references therein.
[37] C.-H. Huang, Biochemistry 8 (1969) 344–352.
[38] D. Sarkar, D. Bose, A. Mahata, D. Ghosh, N. Chattopadhyay, J. Phys. Chem. B 114 (2010) 2261–2269.
[39] C. Ghatak, V.G. Rao, R. Pramanik, S. Sarkar, N. Sarkar, Phys. Chem. Chem. Phys. 13 (2011) 3711–3720.
[40] K. Shiba, T. Niidome, E. Katoh, H. Xiang, L. Han, T. Mori, Y. Katayama, Anal. Sci. 26 (2010) 659–663. and references therein.
[41] C. Rodrigues, P. Gamerio, S. Reis, J.L.F. Lima, B. de Castro, Langmuir 18 (2002) 10231–10236.
[42] A. Coutinho, M. Prieto, Biophys. J. 69 (1995) 2541–2557.
[43] B. Sengupta, A. Banerjee, P.K. Sengupta, FEBS Lett. 570 (2004) 77–81.
[44] A.P. Demchenko, Luminescence 17 (2002) 19–42.
[45] S.K. Patra, M.K. Pal, Spectrochim. Acta 53A (1997) 1609–1614.
[46] A. Samanta, J. Phys. Chem. B 110 (2006) 13704–13716. and references therein.
[47] K. Bhattacharyya, Acc. Chem. Res. 36 (2003) 95–101.
[48] F. Moyano, M.A. Biasutti, J.J. Silber, N.M. Correa, J. Phys. Chem. B 110 (2006) 11838–11846.
[49] E. Oldfield, D. Chapman, FEBS Lett. 23 (1972) 285–297.
[50] G. Maglia, A. Jonckheer, M.D. Maeyer, J.-M. Frere, Y. Engelborghs, Protein Sci. 17 (2008) 352–361.
[51] M.C. Tory, A.R. Merrill, Biochim. Biophys. Acta 1564 (2002) 435–448.
[52] A.S. Klymchenko, Y. Mely, A.P. Demchenko, G. Duportail, Biochim. Biophys. Acta 1665 (2004) 6–19.
[53] C. Richardt, in: H. Ratajazak, W.J. Orville-Thomas (Eds.), Molecular Interaction, vol. 3, Wiley, New York, 1982, p. 255.
[54] Y. Cohen, M. Afri, A.A. Frimer, Chem. Phys. Lipids 155 (2008) 114–119.
[55] J.-L. Bredas, D. Beljonne, V. Coropceanu, J. Cornil, Chem. Rev. 104 (2004) 4971–5004.
[56] C.H. Cho, M. Chung, J. Lee, T. Nguyen, S. Singh, M. Vedamulthu, S. Yao, S.B. Zhu, G.W. Robinson, J. Phys. Chem. 99 (1995) 7806–7812.
[57] G.B. Dutt, J. Phys. Chem. B 108 (2007) 3651–3657. and references therein.
[58] S. Dutta Choudhury, M. Kumbhakar, S. Nath, H. Pal, J. Chem. Phys. 127 (2007) 194901–194913. and references therein.
[59] R.K. Mitra, S.S. Sinha, S.K. Pal, Langmuir 24 (2008) 49–56.
[60] A. Chattopadhyay, S. Mukherjee, Biochemistry 32 (1993) 3804–3811.
[61] E. Perochon, A. Lopez, J.F. Tocanne, Biochemistry 31 (1992) 7672–7682.
[62] A. Chattopadhyay, S. Mukherjee, J. Phys. Chem. B 103 (1999) 8180–8185.
[63] M.N. Jones, Int. J. Pharm. 177 (1999) 137–159.